

Photon localization in a disordered multilayered system

K. M. Yoo and R. R. Alfano

Institute for Ultrafast Spectroscopy and Laser and Photonics Application Laboratory, Department of Physics, The City College of New York, 138th Street and Convent Avenue, New York, New York 10031

(Received 9 June 1988)

Classical wave propagation in random multilayered media has been studied by numerical simulation in terms of interface reflectance, fluctuation of layer thickness, and number of layers. Several interesting features on wave propagation in finite media were obtained.

In well-selected random media, waves may not propagate through because of constructive interference among the multiple-scattered waves. Interference localizes the waves into a finite spatial region.¹ Earlier work on localization concentrated mainly on electron transport in disordered solids.² The observation of weak photon localization³⁻⁵ in polystyrene spheres suspended in water has generated a great deal of interest in the study of photon localization⁶⁻¹² and multiple scattering¹³⁻¹⁷ in a random medium. Several experiments have been performed on the transport of photons in disordered media.^{13,14,18-20} As yet, strong photon localization has not been observed experimentally, even in a one-dimensional random system where both the quantum-mechanical²¹ and classical waves²²⁻²⁴ are known to be localized. The localization length for a one-dimensional random system²³ has been investigated theoretically, and was found to diverge at the Brewster angle for *p*-polarized light.²⁴ In this work, we proceed to investigate numerically the characteristic of wave transmission through random nonabsorbing multilayered systems as a function of interface reflectance, fluctuation of layer thickness, and number of layers, instead of calculating the localization length. The insight presented here could serve as an important guide to the experimentalists searching for a localized system.

Consider a wave incident on a multilayered dielectric random system with alternating refractive indices n_0 and n_1 as shown in Fig. 1. The wave propagation and localization were studied in terms of reflectivity or transmit-

tivity of the system as a function of randomness and dimension (thickness) of the system. The reflectivity of the system is formulated following Rouard's method.^{25,26}

The Fresnel coefficient of the last (*k*th) layer is given by

$$\rho_k e^{-i\Delta_k} = \frac{r_k + r_{k+1} e^{-2i\delta_k}}{1 + r_k r_{k+1} e^{-2i\delta_k}}, \tag{1}$$

where r_k is the reflectance at interface *k* and is given by

$$r_{\text{odd}} = -r_{\text{even}} = \frac{n_0 \cos\theta_0 - n_1 \cos\theta_1}{n_0 \cos\theta_0 + n_1 \cos\theta_1}, \tag{2}$$

where δ_k is the phase shift of the wave at the *k*th layer, θ_0 is the angle of incidence, and θ_1 is the angle of refraction in dielectric layer n_1 . The equation holds for light polarized perpendicular to the plane of incidence.

The phase shift of light propagating through the *k*th layer is directly related to the thickness of the layer d_k by

$$\delta_k = \frac{2\pi n_k d_k}{\lambda \cos\theta_{0,1}}, \tag{3}$$

where n_k is the refractive index of the *k*th layer, and λ is the wavelength in vacuum. The phase shift of the *k*th layer is given by

$$\delta_k = \pi(1 + s\xi_k), \tag{4}$$

where $\xi_k \in [-1, 1]$ are random numbers generated by the computer, and the number *s* sets the range of fluctuation and thus the degree of fluctuation for the phase shift δ_k . The mean phase shift is π . The Fresnel coefficient of the *k*th layer is used to calculate the Fresnel coefficient for the (*k* - 1)th layer as

$$\rho_{k-1} e^{-i\Delta_{k-1}} = \frac{r_{k-1} + \rho_k e^{-i\Delta_k} e^{-2i\delta_{k-1}}}{1 + r_{k-1} \rho_k e^{-i\Delta_k} e^{-2i\delta_{k-1}}}. \tag{5}$$

This process is repeated successively until the first interface where ρ_1 is found. The reflection *R* from the system is given by ρ_1^2 , and the transmission is given by $T = 1 - R$.

An ordered multilayered system is totally transmitting when each layer has the same optical thickness with a phase shift $\delta_k = \pi$. As the optical thickness (δ_k) of each layer increases by the same amount, the reflectivity of the

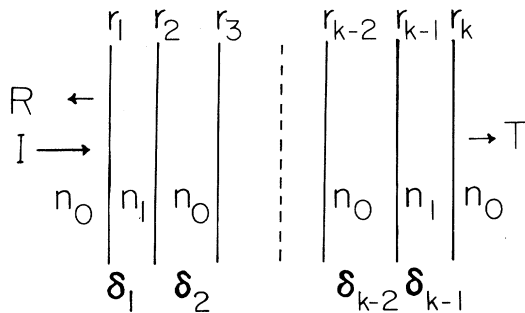


FIG. 1. Multilayers of dielectric films with alternating refractive indices n_0 and n_1 . δ_k is the phase shift of the *k*th layer and r_k is the reflectance at the *k*th interface.

system oscillates between 0 and some small value, and becomes totally reflecting around $\delta_k = \pi + \frac{1}{2}\pi$. Figure 2 shows the well-known feature of reflectivity of the ordered multilayered system. The frequency of the oscillation of the reflectivity is larger for the system with a larger number of layers.

When the thickness of each layer becomes random, the nature of the reflectivity of the system changes drastically. The reflectivity or transmittivity of the random system depends on three parameters of the system: the number of layers n , the fluctuation of layer thickness σ_δ (measured in phase shifts), and the layer interface reflectance r . The dependence on each of these parameters when one parameter is varied and the other two are kept constant will be pursued in the following sections.

As the thickness (number of layers) of the random system increases, the transmittivity fluctuates wildly and eventually decreases to zero as shown in Fig. 3. The transmission curve shown in dots is the ensemble average of 300 transmission curves, where each curve has the same σ_δ but with a distinct set of random numbers for the phase shift δ_k . The salient feature of the transmission curve is that it cannot be fitted by a single exponential function. Initially, the transmission decays exponentially until the thickness of the system reaches the localization length above which the transmission decays almost linearly. The initial exponential decay could be confused with absorption in the medium in optical transmission experiment.

The error bars drawn on the curve in Fig. 3 are the standard deviations computed from the set of 300 individual systems without ensemble averaging. These large error bars indicate that the transmissions vary widely in each of these individual systems. Although they have the same σ_δ but a distinct set of δ . This large variation from system to system is a typical characteristic of a random system. However, the transmission curve from a system with ensemble averaging over a large number of systems is well behaved; that is, the ensemble average of one system differs very slightly from another ensemble-averaged

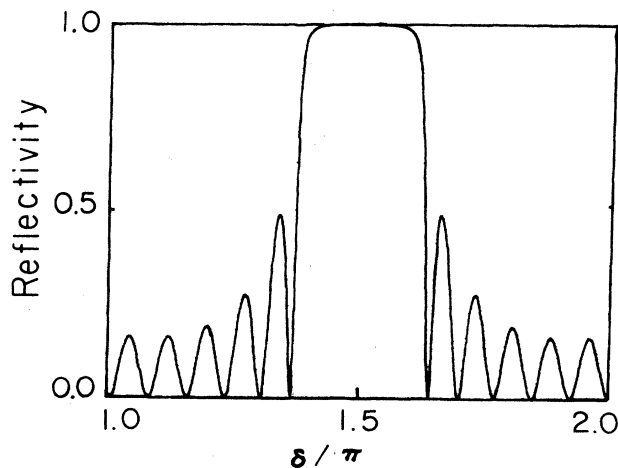


FIG. 2. The reflectivity of an ordered multilayered system as a function of layer thickness (δ). Number of layers, $n=10$; interface reflectance, $r=0.4$.

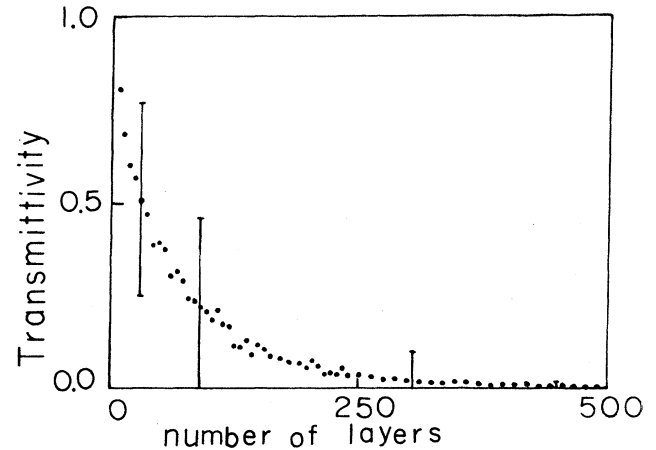


FIG. 3. The transmission (300 ensemble average) as a function of the number of layers. $r=0.4$, $\sigma_\delta=0.12\pi$. The error bars indicate the degree of fluctuation for the individual system.

system. The discussion here also applies to the large error bars in Figs. 4 and 6.

The reflectivity of the disordered system as a function of randomness of the layer thickness is investigated next. The randomness is measured in terms of the standard deviation of layer phase shift σ_δ . After ensemble averaging of 100 sets of data, the reflectivity curve is rather smooth and differs slightly from curve to curve. The general behavior of reflectivity as σ_δ increases is displayed by the curves for four different thicknesses which are plotted in Fig. 4. For all these systems, the initial increase in reflectivity is very slow as σ_δ is increased from zero up to a certain value, for example, $\sigma_\delta \approx 0.1\pi$ for a system with 50 layers. This value is smaller for systems with a larger number of layers or larger interface reflectance. Above this value, the reflectivity increase linearly. The gradient

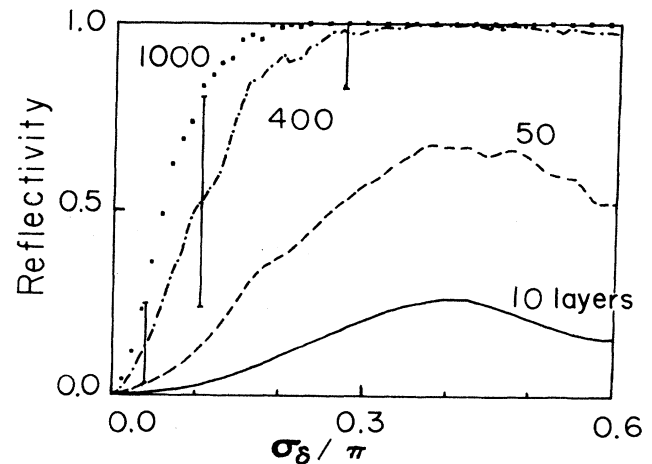


FIG. 4. The reflectivity (100 ensemble average) as a function of the standard deviation of layer thickness in terms of phase shift. The main phase shift is π . Reflectance, $r=0.15$; different curves correspond to a different number of layers as indicated.

of the linear portion of the curve yields important information on whether or not, with larger fluctuations, the localization length can become smaller than the thickness of the system, a condition where the system becomes opaque. The critical gradient (m_c) for the slope is found to be about 2.7. Above this value the system will eventually become opaque as σ_δ is increased further, although the interface reflectance and number of layers remain the same. For systems with gradient $m < m_c (=2.7)$, the maximum reflectivity (minimum transmission) occurs at $\sigma_\delta \approx 0.4\pi$. The reflectivity oscillates about a constant value as the σ_δ is increased further.

For an individual system, without ensemble averaging, the reflectivity fluctuates with sharp spikes as s (and σ_δ) increases, see Figs. 5(a) and 5(b). These figures show that the reflectivity differs markedly with different sets of random variables for phase shift, for the systems having the same σ_δ, n , and r . The systems with gradient $m < 2.7$ (gradient of the ensemble-averaged system) are shown in

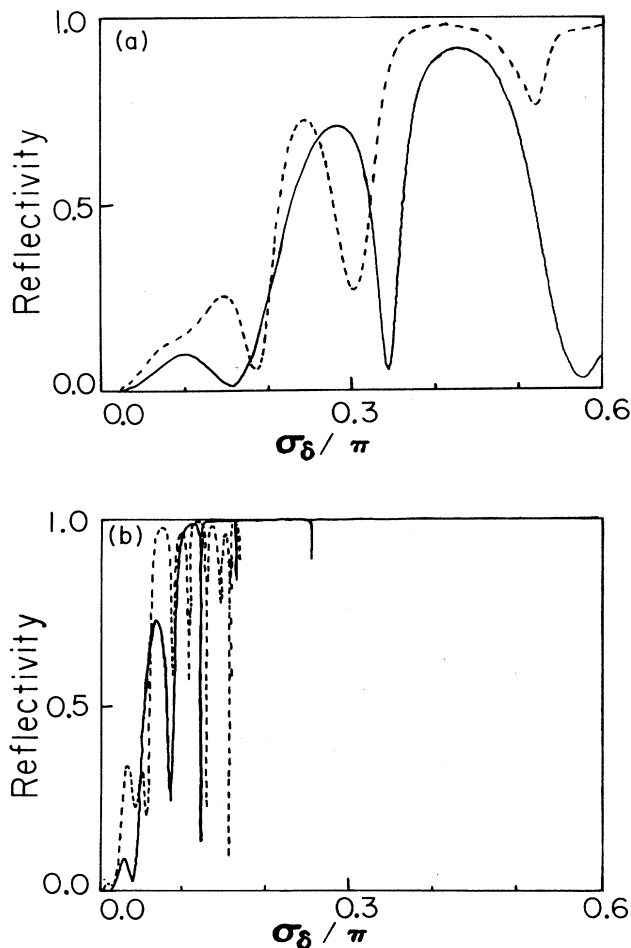


FIG. 5. (a) Reflectivity vs σ_δ , $r=0.15$ and 50 layers. Two curves are shown, each with a different set of random variables for the phase shift. (b) Reflectivity vs σ_δ , $r=0.15$ and 1000 layers. Two curves are shown, each with a different set of random variables for the phase shift.

Fig. 5(a) and they will never become opaque for any choice of σ_δ , whereas system with $m > 2.7$ (with ensemble averaging) become opaque when σ_δ is above a certain value, as shown in Fig. 5(b). The salient feature of all the curves shown in Fig. 5 is that the reflectivity remains small as σ_δ increases from zero, and then suddenly surges as σ_δ increases above certain values. This feature is similar to a recent experimental observation involved with electron transport in random superlattices. In that experiment, the photoluminescence²⁷ from a quantum well sandwiched between disordered superlattices decreased abruptly when the fluctuation of the layer thickness of the superlattice increased to a certain value.

Finally, the reflectivity is studied as a function of layer interface reflectance r . The general behavior of the reflectivity after an ensemble average over a large number of data sets is summarized by the curves displayed in Fig. 6. The reflectivity first increases slowly, then linearly, and becomes slower as the reflectivity approaches unity. The curves in Fig. 7 serve to illustrate that the reflectivity differs markedly for different sets of random variables, even though each set of these variables contribute the same standard deviation for the phase shift σ_δ . These individual curves also show some broad and sharp spikes. The salient features displayed on curves in Figs. 6 and 7 are similar to those displayed in Figs. 4 and 5, respectively. This similarity is expected since the reflectivity increases with randomness, either from large fluctuation of layer thickness or interface reflectance.

Strong photon localization can easily be achieved with present thin-film fabrication technology and dielectric materials. In the visible region, materials with a high-refractive-index contrast, namely zinc sulfide ($n \approx 2.35$) and cryolite ($n \approx 1.35$), which give $r=0.27$, can be fabricated in an alternating multilayer system with $\sigma_\delta \approx 0.51\pi$. This system with 50 layers can yield 90% reflectivity, and with 320 layers completely reflects the incident light. A better system might be fabricated from

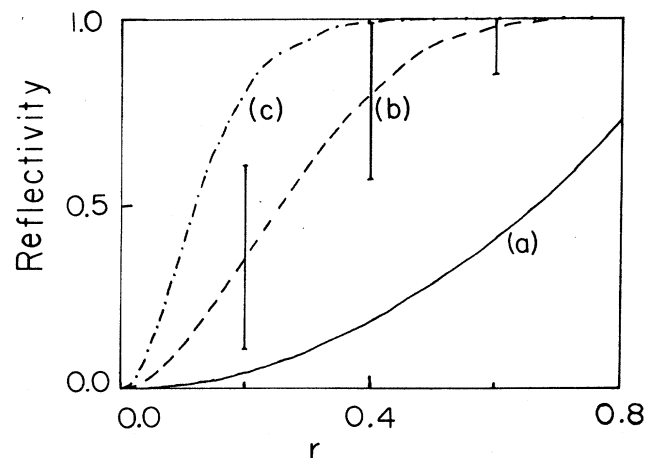


FIG. 6. Reflectivity (100 ensemble average) vs interface reflectance r with three different σ_δ : (a) 0.027π , (b) 0.11π , and (c) 0.23π . The mean phase shift is $\delta = \pi$ and 100 layers.

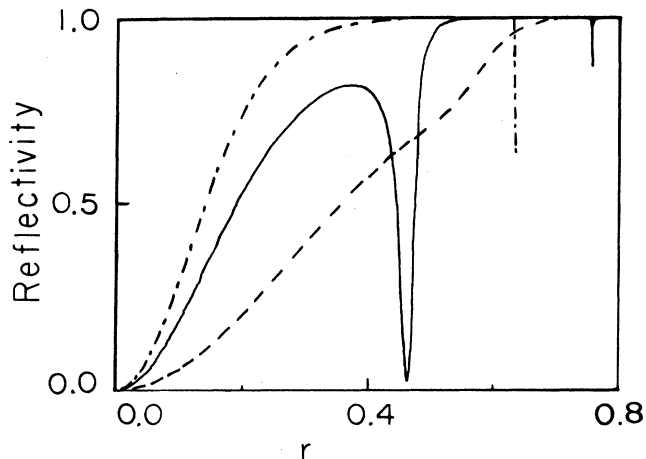


FIG. 7. Reflectivity vs interface reflectance r , mean $\delta = \pi$, and 100 layers. Three curves are shown, each with a different set of random variables but having the same standard deviation $\sigma_\delta = 0.11\pi$, and the ensemble average of 100 is shown in Fig. 6, curve (b).

infrared materials where a significantly higher-refractive-index contrast can be obtained, e.g., lead telluride ($n \approx 5.5$) and silicon monoxide ($n \approx 1.7$), which can be fabricated with a much smaller number of layers to yield photon localization. Only the system with 10 layers with $\sigma_\delta \approx 0.51\pi$ yields 90% reflectivity, and with 80 layers completely reflects the wave.

In summary, photon propagation in nonabsorbing disordered multilayer systems has been studied as a function of different system variables. For systems with ensemble averaging, the transmission of a wave through a system of random multilayers decreases exponentially and then decreases more slowly as the number of layers increases. The random system has a maximum reflectivity when the fluctuation of layer thickness is around $\sigma_\delta \approx 0.4\pi$. For systems with small fluctuations, there is a range in which the reflectivity increases linearly with σ_δ . If the gradient of this linear increase is greater than the critical gradient of 2.7, then the system can become opaque for some larger σ_δ , with the interface reflectance and the number of layers remaining the same. For systems without ensemble averaging, a large fluctuation of reflectivity with sharp spikes as randomness increases is expected and shows a sudden surge in reflectivity as the randomness increases from zero. The features presented above and photon localization are shown to be easily observed experimentally in random multilayered systems.

K. M. Yoo would like to acknowledge the Physics Department of the City College of New York and the Graduate Center of the City University of New York (CUNY) for financial support. This research is supported in part by Hamamatsu Photonic K.K. and the Professional Staff Congress (PSC/CUNY).

- ¹P. W. Anderson, *Phys. Rev.* **109**, 1492 (1958).
- ²Nevill Mott, *J. Phys. C* **20**, 3075 (1987); *Prog. Theor. Phys. Suppl.* **84**, 1 (1985).
- ³Y. Kuga and A. Ishimaru, *J. Opt. Soc. Am. A* **8**, 831 (1984).
- ⁴Meint P. Van Albada and Ad Lagendijk, *Phys. Rev. Lett.* **55**, 2692 (1985).
- ⁵Pierre-Etienne Wolf and Georg Maret, *Phys. Rev. Lett.* **55**, 2696 (1986).
- ⁶Sajeev John, *Phys. Rev. Lett.* **53**, 2169 (1984).
- ⁷Ping Sheng and Zhao-Qing Zhang, *Phys. Rev. Lett.* **57**, 1879 (1986).
- ⁸K. Arya, Z. B. Su, and Joseph L. Birman, *Phys. Rev. Lett.* **57**, 2725 (1986).
- ⁹Ping Sheng, Zhao-Qing Zhang, Benjamin White, and Georg Papanicolaou, *Phys. Rev. Lett.* **57**, 1000 (1987).
- ¹⁰Sajeev John, *Phys. Rev. Lett.* **58**, 2486 (1987).
- ¹¹Mahito Kohmoto, Bill Sutherland, and K. Iguchi, *Phys. Rev. Lett.* **58**, 2436 (1987).
- ¹²Benjamin White, Ping Sheng, Zhao-Qing Zhang, and Georg Papanicolaou, *Phys. Rev. Lett.* **59**, 1918 (1987).
- ¹³S. Etamad, R. Thompson, and M. J. Andrejco, *Phys. Rev. Lett.* **57**, 575 (1986).
- ¹⁴M. Kaveh, M. Rosenbluh, I. Edrei, and I. Freund, *Phys. Rev. Lett.* **57**, 2049 (1986).
- ¹⁵Michael J. Stephen, *Phys. Rev. Lett.* **56**, 1809 (1986).
- ¹⁶B. Shapiro, *Phys. Rev. Lett.* **57**, 2168 (1986).
- ¹⁷V. A. Davis, and L. Schwartz, *Phys. Rev. B* **31**, 5155 (1985).
- ¹⁸G. H. Watson, Jr., P. A. Fleury, and S. L. McCall, *Phys. Rev. Lett.* **58**, 945 (1987).
- ¹⁹K. M. Yoo, K. Arya, G. C. Tang, Joseph L. Birman, and R. R. Alfano, *Phys. Rev. A* (to be published).
- ²⁰Azriel Z. Genack, *Phys. Rev. Lett.* **58**, 2049 (1987).
- ²¹E. Abrahams, P. W. Anderson, D. C. Licciardello, and T. V. Ramakrishnan, *Phys. Rev. Lett.* **42**, 673 (1979).
- ²²M. Matsuda and K. Ishii, *Prog. Theor. Phys. Suppl.* **45**, 56 (1970).
- ²³P. Sheng, B. White, Z. Q. Zhang, and G. Papanicolaou, *Phys. Rev. B* **34**, 4757 (1986).
- ²⁴J. E. Sipe, P. Sheng, B. S. White, and M. H. Cohen, *Phys. Rev. Lett.* **60**, 108 (1988).
- ²⁵P. Rouard, *Ann. Phys. (Paris)* **7**, 291 (1937).
- ²⁶O. S. Heavens, *Optical Properties of Thin Solid Films* (Academic, New York, 1955), pp. 63–65.
- ²⁷A. Chomette, B. Deveaud, A. Regreny, and G. Bastard, *Phys. Rev. Lett.* **57**, 1464 (1986).